

QC
880
.A4
no.76/16

Environmental Research Laboratories

Air Resources

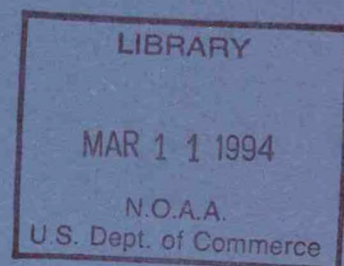
Atmospheric Turbulence and Diffusion Laboratory

Oak Ridge, Tennessee

Spring 1977

THE DISTRIBUTION OF SOLAR RADIATION WITHIN A DECIDUOUS FOREST

Boyd A. Hutchison and Detlef R. Matt



U. S. DEPARTMENT OF COMMERCE
NATIONAL OCEANIC AND ATMOSPHERIC ADMINISTRATION

ATDL Contribution File No. 76/16

QC
880
M
no. 76/16

THE DISTRIBUTION OF SOLAR RADIATION WITHIN A DECIDUOUS FOREST¹

BOYD A. HUTCHISON
AND

DETLEF R. MATT

Atmospheric Turbulence and Diffusion Laboratory, National Oceanic and Atmospheric Administration, P.O. Box E, Oak Ridge, Tennessee 37830 USA

MAR 11 1994

N.O.A.A.
Dept. of Commerce

Abstract. Solar radiation was measured within and above an east Tennessee deciduous forest over a 2-yr period. Diurnal patterns of within-forest radiation follow the temporal variation in incident radiation but become more irregular with depth in the forest because of the highly variable penetration of beam radiation in space and in time. Seasonally, radiation in the forest increases substantially from winter to its annual maximum in early spring as solar elevations increase. Although solar elevations continue to rise each day until the summer solstice, amounts of total radiation and its beam component drop sharply in the forest with the advent of leaf expansion. Diffuse radiation in the forest continues to increase slowly following the onset of leaf expansion but reverses as the forest approaches a fully leafed state. Following the summer solstice, forest structure remains essentially static until abscission while solar elevations decrease. In summer and early autumn, total radiation and both its beam and diffuse components decrease slowly in the forest to their annual minimum in autumn. With leaf abscission and subsequent fall, radiation increases slightly in the forest but soon declines again as solar elevations approach their annual minimum of the winter solstice.

Key words: Deciduous forest; diffuse radiation; direct beam radiation; diurnal variation; fractional penetration; radiation climate; seasonal variation; solar radiation; spatial variation; temperate forest; Tennessee.

INTRODUCTION

Solar energy is the driving force for essentially all processes occurring within ecosystems. Because of the dependence of ecosystem functioning upon solar energy, evolution has resulted in ecosystems that tend to be dominated by the primary producer trophic level. In terrestrial ecosystems, green plants are nearly always the ecological dominants. By virtue of the architecture of forest ecosystems, the canopy of photosynthetic tissue largely governs both abiotic and biotic energy flows within these ecosystems. The canopy controls abiotic energy flow through the combined effects of biomass distribution, geometry, and optical characteristics upon the penetration of solar radiation into the forest and upon the partitioning of radiant energy within the forest. Since forest canopies shade the ground beneath, the bulk of photosynthetic production of forests occurs in the overstory canopy, therefore the biotic energy flow in the system is strongly controlled as well.

As part of the ecosystem analysis effort at the Oak Ridge site, Eastern Deciduous Forest Biome, U.S. International Biological Program, we have studied the space and time distribution of solar radiation within a deciduous forest dominated by tulip poplar (*Liriodendron tulipifera*). The objectives of this

study were: (1) to determine the variation of solar radiation in space and time in the forest and (2) to relate this variation to the structure and phenological state of the forest. In this paper we deal with these objectives rather qualitatively. Subsequent papers will attempt to quantify the relationships between forest radiation regimes and forest structure.

Forest radiation regimes are highly variable because of the interactions of a variety of external and internal factors. Amounts of radiation incident upon the forest vary regularly owing to diurnal and seasonal changes in earth-sun geometry and irregularly because of varying atmospheric turbidity and cloudiness. Optical characteristics of forests change through time with phenological changes in forest structure and with forest tree growth. Superimposed upon the variation produced by these factors is that variability resulting from horizontal and vertical heterogeneity in forest structure.

In this paper we illustrate the effects of the earth's daily rotation upon forest radiation regimes by considering full-day radiation records above and within the forest. The effects of seasonal changes in earth-sun geometry and of phenological changes in forest structure are shown by comparing clear-day radiation totals in each of seven phenoseasons which characterize the forest in terms of season and phenological state. A phenoseason is a segment of the year during which the prevailing earth-sun geometry and pheno-

¹Manuscript received 31 October 1975; accepted 28 December 1976.

TABLE 1. Mensurational data and diversity of the cesium-tagged *Liriodendron* forest at the Oak Ridge site

| Canopy level | Height (m) | Average dbh (cm) | Basal area (m ² /hectare) | Density (stems/hectare) | Shannon-Weaver species diversity index |
|--------------|--------------|------------------|--------------------------------------|-------------------------|--|
| Upper | 16-30 | 23.8 | 24.0 | 520 | 1.11 |
| Mid | 10-15 | 8.6 | 1.7 | 290 | 1.42 |
| Forest floor | 1.5- 9 | 2.3 | 3.0 | 4770 | 1.78 |
| Overall | Range 1.5-30 | — | Total 28.7 | Total 5580 | Overall index 2.06 |

logical state of the forest create a unique set of conditions which determine forest radiation regimes. We present data from clear days to prevent confounding the effects of these sources of variation by changing cloudiness. Nevertheless, some variation is included resulting from the differing amounts of atmospheric turbidity present on these clear days. Since we have no measure of this factor, we are unable to separate out its effect upon forest radiation other than by selecting data from the clearest days of record for analysis. To show the effect of cloud cover, we include data from a heavily overcast day in winter and in summer for comparison. Since partly cloudy days are difficult to characterize for comparative purposes, we ignore data from such days except in the derivation of the annual radiation budget for the forest under study. Finally, the effects of horizontal and vertical heterogeneity in forest structure are quantified through replication of measurements of forest radiation in horizontal and vertical space.

To further illustrate the effects of seasonality and phenological changes in forest structure, average phenoseasonal penetration rates were calculated and applied to phenoseasonal total incident radiation measured at the NOAA weather station in Oak Ridge, 10 km to the north. As described below, the method of derivation of the seasonal budget attempts to account for the variation arising from differing degrees of cloudiness and morning fog that is frequently present in east Tennessee. All data from this study are written on magnetic tape and may be obtained for further analysis from the authors.

SITE DESCRIPTION

The forest in which this study of radiation climate was made is a seral, deciduous forest composed predominantly of tulip poplar, *Liriodendron tulipifera* L. The stand is ≈50 yr of age and is situated in a moist limestone sink on the ERDA reservation ≈10 km south of the town of Oak Ridge. Because of the mesic nature of the sink, this stand has a higher density and a more highly developed understory than is typical of the Appalachian region.

The overstory canopy is nearly pure tulip poplar although numerous other species are present in small numbers. The overstory canopy extends down past the zone of crown closure (=20 m above the floor) to about 16 m elevation. The lower limit of the overstory is rather well defined since the live crown generally ends at 16 m. Between 16 and 10 m there are a few crowns of suppressed trees, but in general this stratum is devoid of biomass other than the boles of codominant overstory trees. Below 10 m, however, is a rather distinct secondary canopy composed principally of flowering dogwood (*Cornus florida*) and redbud (*Cercis canadensis*). This secondary canopy extends down to about 3 m above the forest floor. Below 3 m are the crowns of numerous saplings and shrubs of various species.

The pertinent mensurational data for this forest are shown in Table 1, along with the Shannon-Weaver diversity indexes for tree species in the various canopy strata. The overall basal area of this forest at the time of this study was ≈28 m²/ha, while the total stem density exceeded 5,500 stems/hectare. The leaf area index of this forest when fully leafed was 6.0 (Dinger et al. 1972). Figure 1 shows a general view of the forest under study in summer full-leaf.

The climate of the region in which the study site is situated is characteristically warm and humid. Winters are mild and wet with frontal storm systems predominating. Summers are hot and humid with convective thunderstorms developing almost daily, yielding scattered areas of intense precipitation. Because of the high humidity and nearby reservoirs in the Tennessee River system, heavy radiative ground fog is frequently present in mornings throughout the year. Hence, fog at this site often persists well into the day.

The study is within the zone of influence of an unshielded research reactor at the Oak Ridge National Laboratory. Because of this, we could enter the site only during periods when the reactor was not in operation. As a result, instruments and the data acquisition system could not be checked frequently, hence, maintenance and repair of the monitoring



FIG. 1. General view of the tulip poplar stand in midsummer showing method of deployment of elevated solarimeters. ORNL Photo #2155-73.

system was a continuing problem which created difficulties in data analysis.

METHODS

Radiation reaching the earth's surface is of two forms; radiation in a collimated beam directly from the sun (beam radiation), and radiation diffused by its passage through the earth's atmosphere (diffuse or sky radiation). These two radiative components interact differently with vegetation and so must be measured separately if the relationships between stand structure and radiation climate are of interest (Anderson 1964b). Total radiation was measured using open sensors, while the diffuse component was measured using sensors equipped with shadow bands as designed by Horowitz (1969). (A shadow band is visible on the forest floor in Fig. 1.) Subtracting the diffuse radiation amount from the simultaneous total radiation yields an estimate of the direct beam radiation received at that time.

The penetration of beam radiation into a forest depends upon the flux density of the solar beam incident upon the stand and upon the number, size, and space distribution of canopy openings (Anderson 1964c, Anderson and Denmead 1969, Horn 1971, Reifsnyder et al. 1971). On the other hand, diffuse radiation penetration depends upon the distribution and amount of sky brightness, the number, the size, and the space distribution of canopy openings, and the geometry, space distribution, and optical characteristics of the forest biomass (Verhagen et al. 1963, Anderson 1964b,c, Anderson and Denmead 1969, Horn 1971, Miller and Norman 1971). Since the sun's apparent position changes through the day and from day to day, and since canopy opening distributions tend to be highly variable, the amount of beam radiation penetrating a forest canopy is highly variable in space and time. In contrast, the factors governing the penetration of diffuse radiation are not highly variable, therefore diffuse radiation within a forest is more uniform in space and time. As a result, different sampling schemes are necessary for measurements of the two radiative components if comparable statistical accuracy of the two quantities is required (Gay et al. 1971, Reifsnyder et al. 1971). Reifsnyder et al. (1971) found that 18 replicate measurements of total radiation at the floor of a Connecticut deciduous forest were necessary to obtain space means having standard errors of the means of ± 10 milliangles per minute (mly/min) [≈ 418 joules/m²] or less. Only two replications of the diffuse measurement were necessary to attain this level of precision.

Radiant flux densities were measured within and above the forest with an array of Lintronic Dome Solarimeters®, a commercial modification of Mon-

teith's (1959) field solarimeter. These instruments sense radiation in the spectral band 0.3 to 3 μm , this band accounting for some 98% of the solar energy reaching the earth's surface (Fritz 1958). Horizontal space variation in total radiation received within the forest was assessed through replication of observations at a given level. Vertical variation was similarly determined by replicating the horizontal arrays at three levels in the forest. All sensors were randomly situated in horizontal space with 11 replications at the 16-m level and 12 at the 3- and 0-m levels. Elevated sensors were mounted on the tops of telescoping steel masts extended to the desired height (see Fig. 1).

The levels of vertical replications of measurement were selected such that the attenuation of radiation by major canopy strata could be determined. The sensors at 16 m were at the base of the overstory canopy while those at 3 m were at the base of the secondary canopy. The sensors on the forest floor were elevated above the general level of herbaceous vegetation and thus sensed that radiation penetrating the three-canopy strata: the overstory canopy, the secondary understory canopy, and the shrub layer.

Incoming diffuse radiation was also measured at each of these levels. Following Reifsnyder et al. (1971), the diffuse measurements were replicated twice at the 0- and 3-m levels. Only one measurement of this variable was possible at 16 m throughout 1972 and early 1973. In late 1973, the diffuse measurement was replicated twice at 16 m as at other levels.

The total and diffuse radiation incident upon the forest was measured using single open and shaded sensors located 32 m above the forest floor, 1 to 2 m above the tops of the tallest trees. Although Drummond (1956) developed a method for correcting measurements of diffuse radiation for that radiation originating in the area of sky occluded by the shadow band, all diffuse data are presented here uncorrected. We feel that the distribution of brightness in the forest canopy is likely to be considerably different from that in the sky owing to the conversion of beam radiation to diffuse radiation by multiple reflections and transmissions from and through leaves. Hence application of corrections such as those proposed by Drummond (1956) is probably inappropriate for measurements within plant stands and thus all diffuse data are presented in their uncorrected form.

All sensors were periodically recalibrated against an Eppley Precision Pyranometer® that we use as a local standard. Owing to the nonlinear response of the Lintronic sensors, nonlinear calibration functions were empirically derived for each sensor used in this study (Matt and Hutchison 1974). These functions were used to convert the millivolt output signals from the Lintronic solarimeters to engineering units. Care was taken to orient all sensors the same during cali-

bration and during field measurements to minimize errors arising from departures from flatness of the printed-circuit sensing elements.

The output signals from all sensors were fed into a data acquisition system, scanned periodically (10-min intervals on weekdays in 1972, 5-min intervals on weekdays in 1973, and 20-min intervals on weekends), converted to digital form, and recorded on punch paper tape. Subsequently these paper tapes were read, the data converted to engineering units, edited, and summarized.

As noted above, horizontal space variation in total and diffuse radiation was assessed through simultaneous, horizontally replicated measurements. The space average direct beam radiation can then be derived by subtracting the space mean diffuse radiation from the space mean total. Vertical variation was assessed through comparison of space means from the three different levels. Temporal variation within days was characterized by analyzing radiation measurements made periodically through full days. All curves of smoothed data were smoothed using a five-point smoothing technique.

Seasonal variation in radiation incident upon the earth's surface increases with increasing latitude owing to the combined effects of the earth's tilted axis of rotation and its annual revolution about the sun. Superimposed upon this regular, annual cycle of radiation received within plant stands is another, less regular variation produced by phenological changes in stand structure. Even in temperate zone conifer forests, seasonal changes in radiation climates have been reported which are ascribed to phenological changes in the canopy structure (e.g., Schomaker 1968).

In deciduous forests, the effects of phenological change upon radiation climates within the forests rival those effects of changing celestial geometry. Salisbury (1916) referred to two different radiation climates in the deciduous woodlands in which he worked. The radiation regime in the leafless winter forest was termed the light phase, while the radiation climate of the fully-leaved summer forest was termed the shade phase. While these relative phases are clearcut, they do not coincide with absolute amounts of radiation penetrating deciduous forests because of the great variation in incident insolation from day to day and from season to season (Anderson 1964b).

To account for the seasonally and phenologically induced changes in forest radiation regimes, we define seven phenoseasons as shown in Fig. 2, using the solstices, the equinoxes, and dates of phenological events in this forest of importance to radiation penetration. Phenological data were obtained from Taylor (1974). Data from a single clear day in each phenoseason were summarized and plotted over time of

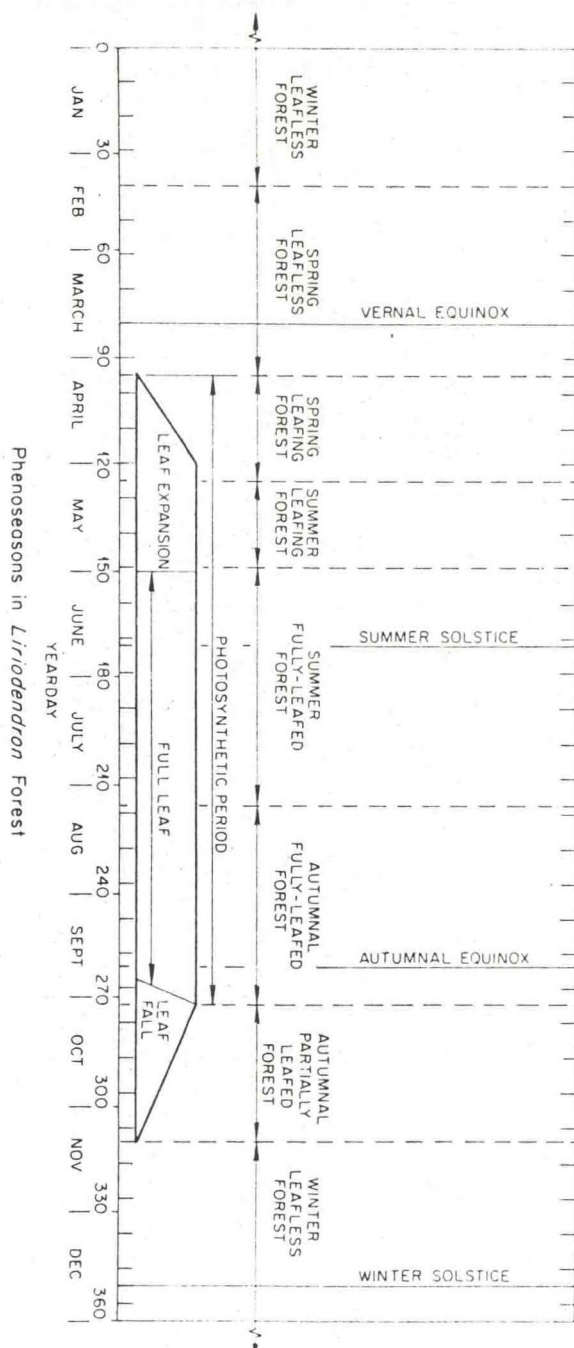


FIG. 2. Phenoseasons in the tulip poplar forest. ORNL Dwg. 74-11562.

year to illustrate the changes in forest radiation climates resulting from changing earth-sun geometry and phenological state.

To further illustrate seasonal differences, average phenoseasonal penetration rates were calculated and applied to the continuous radiation record from the NOAA weather station in Oak Ridge. In this way, the annual radiation regime above and within this

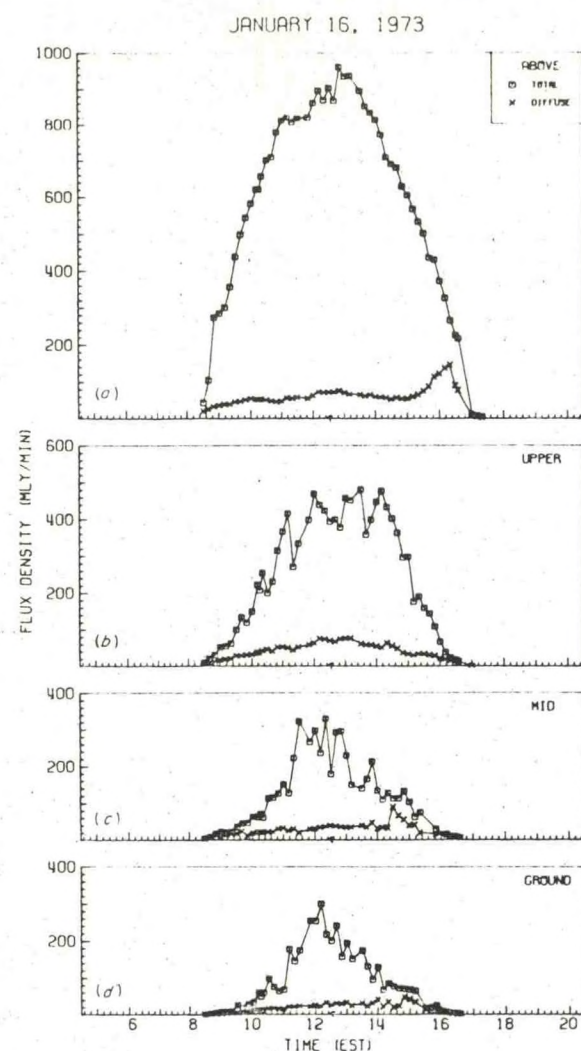


FIG. 3. Diurnal course of average radiation on a clear day in the winter leafless forest: (a) above canopy total and diffuse radiation, (b) 16 m total and diffuse radiation, (c) 3 m total and diffuse radiation, and (d) 0 m total diffuse radiation. The arrows on the abscissae (time axis) of this and subsequent figures denote solar noon. Afternoon peaks in diffuse radiation curves are spurious and result from beam radiation passing beneath the shadow band and striking the shaded sensor. To convert millilangleys (mly) to joules per square metre (J/m^2), multiply by 41.84. ORNL Dwg. 76-15807.

forest was derived. For this approximation, data from partly cloudy days had to be included since partly cloudy skies are far more common than either clear or heavily overcast skies. To incorporate the effects of varying cloudiness, the continuous radiation record from the Oak Ridge weather station was segregated into clear, partly cloudy, and overcast mornings and afternoons and the half-day totals of radiation calculated for each of the six cloudiness time period categories. The separation of morning and

afternoon data was necessary because of the frequent, heavy morning fog that is present in this region on clear to partly cloudy days.

Similarly, the forest radiation data were segregated as above as well as by phenoseason. Average phenoseasonal penetration rates were then calculated for each cloudiness-time period category for each of the three levels in the forest. Summing the appropriate half-day radiation totals from the Oak Ridge station over the phenoseason and multiplying by the corresponding fractional penetration for each forest level yielded an estimate of the total radiation received at each level in the forest for each kind of half-day cloudiness category in each phenoseason. Summing these estimates over all cloudiness classes and half-days in each phenoseason yielded an estimate of the total radiation received during each of seven phenoseasons at each of the three levels in the forest. From these derived totals, gross phenoseasonal mean penetration rates were calculated, as well as photosynthetically active and leafless seasonal totals and percentages.

RESULTS AND DISCUSSION

Clear day forest radiation regimes

Radiation regimes above and within the winter leafless forest on a representative January day are shown in Fig. 3. Since total radiation represents the sum of the beam and diffuse radiation components, the differences between the total and diffuse radiation curves on this and subsequent similar figures represent the flux densities of beam radiation received. As is evident from Fig. 3a, skies on this winter day were clear except for the 2-h period just prior to solar noon. During this time, thin clouds or haze developed which were sufficiently dense to reduce beam radiation inputs slightly, but not so dense as to significantly increase the incident diffuse radiation. The brief plateau at 0900 h in the total radiation record of Fig. 3a results from melting of frost on the solarimeter dome. Peaks in the diffuse radiation records at around 1600 h are spurious and result from beam radiation passing beneath the shadow bands and striking the shaded sensors. The equivalent morning peaks are absent because of topographic shading by a low ridge to the southeast of the study site on this midwinter day.

The rapid morning rise and equivalent rapid afternoon decrease in total radiant flux densities of Fig. 3a are characteristic of reasonably clear day records. Within the leafless forest however (Fig. 3b,c, and d), when solar elevations are low the slopes of the total radiation curves are much reduced from those above the forest. Then at some time nearer solar noon, the slopes of the within-forest curves increase. Through-

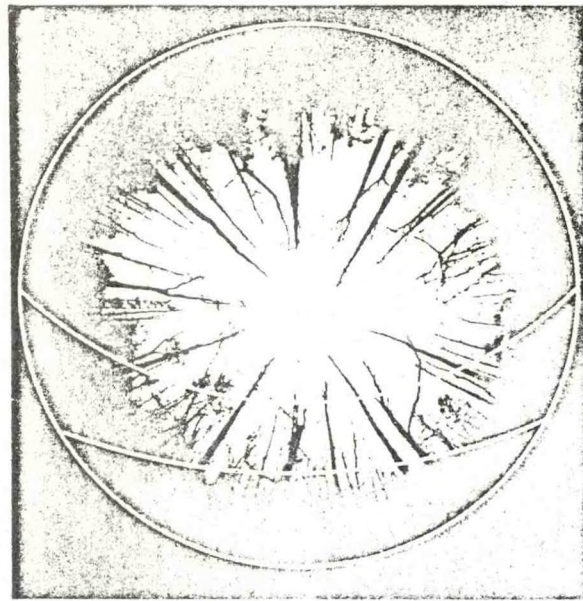


FIG. 4. Canopy photograph of winter leafless forest taken from the forest floor, showing solar paths on the winter solstice and on the vernal equinox. Note that the canopy density is much higher along the winter solstice solar path throughout most of the day than on the vernal equinox, represented by the innermost solar path on this figure. ORNL Photo # 0060-75.

out the day, the slopes of diffuse radiation curves are quite low and change only slowly with time. Hence it is the beam radiative component that is responsible for the changing slopes and temporal irregularity of the total radiation curves.

Figure 4 explains this well. Throughout most of the winter day, the solar path (outermost arc) is obscured by woody forest biomass. Only around midday is sky along the solar path visible from the forest floor. Hence the beam radiation is strongly attenuated by the woody biomass and only at midday can such radiation penetrate to the forest floor. Diffuse radiation, on the other hand, originates from the entire hemisphere of sky and therefore can penetrate into the forest more freely. Note too that as the solar paths rise in the sky from winter to spring, the amount of sky obscured by woody biomass along these paths decreases. Furthermore, the midday period during which the sun is above the completely occluded regions near the horizon lengthens. This has great significance to the seasonal variation in the radiation climates of this forest as is discussed in the seasonal variation section.

While the above canopy record of total radiation appears fairly symmetric about solar noon, the within-forest records show considerable asymmetry. Despite the random siting of replicated sensors in the forest, the heterogeneity of the forest structure is

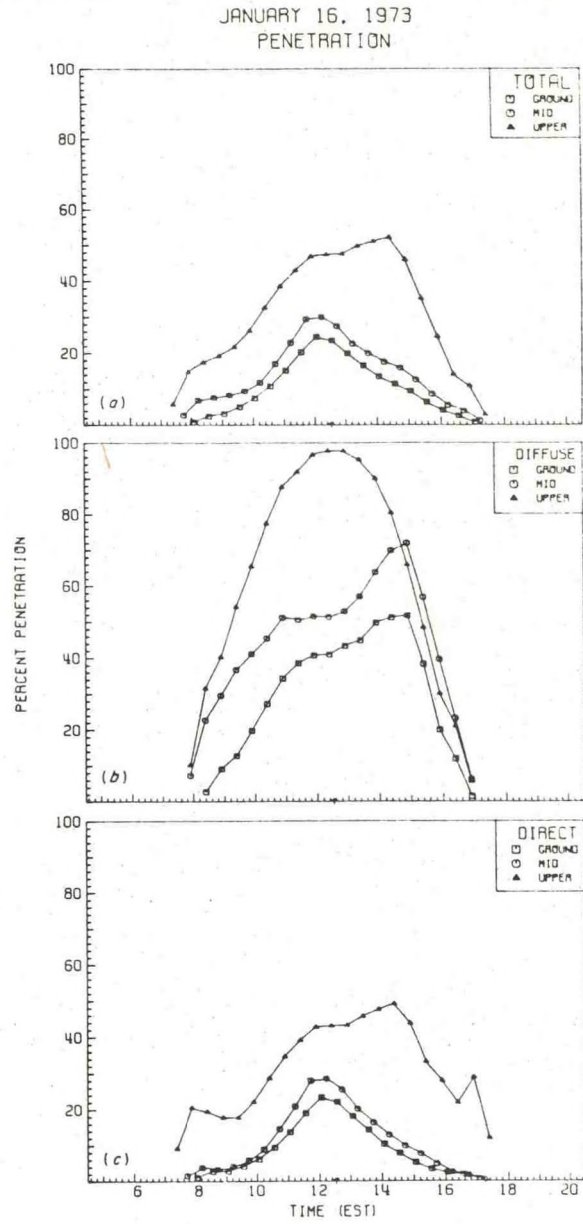


FIG. 5. Smoothed daily course of average fractional penetration of solar radiation in the winter leafless forest under clear skies: (a) total radiation, (b) diffuse radiation, and (c) direct beam radiation. A five-point smoothing technique was used to reduce noise in all smoothed curves. ORNL Dwg. 76-16854.

still manifest in these data. At 16 m, somewhat greater canopy opening is indicated to the west of the sensors at that level. At the 3- and 0-m levels, more canopy openings fall to the east of the sensors than to the west resulting in greater morning penetration of beam radiation. Figure 5 gives further evidence of this. While the fractional diffuse penetrations along with the fractional penetrations of the

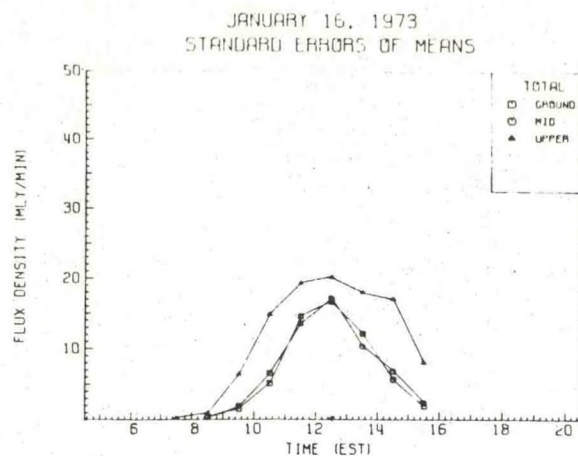


FIG. 6. Smoothed daily course of spatial variability of total radiation received within the winter leafless forest as measured by the half-hour time averaged instantaneous standard error of the space mean total radiation. To convert millilangleys to joules/m², multiply by 41.84. ORNL Dwg. 76-158000.

derived beam radiative component are in error after about 1500 h because of the spurious peaks in the diffuse records of Fig. 3, considerable asymmetry is still evident in Fig. 5 prior to this time. Peak direct beam penetration occurs in midafternoon at 16 m and in late morning at 3- and 0-m levels (Fig. 5c). Since the beam radiation component dominates the total radiation received in the winter forest, the fractional penetration of total radiation (Fig. 5a) follows that of the beam radiation closely.

The penetration of diffuse radiation into the forest exceeds that of the beam component throughout much of the day (Fig. 5b). This would be expected in view of the canopy structure shown in Fig. 4. Greatest attenuation of the beam component occurs in the overstory canopy (Fig. 5c) with much less but still significant attenuation between 16 and 3 m. Little further attenuation between 3 m and the forest floor is indicated. Attenuation of the diffuse component is more even throughout the vertical extent of the forest (Fig. 5b).

Spatial variation in total radiation flux densities within the forest follow the temporal pattern of beam radiation closely (Fig. 6). The space variation is greatest at 16 m and similar in magnitude at the lower levels. Midday variations at all levels greatly exceed the ± 10 -mly/min variation desirable for most energy budget determinations (Reifsnyder et al. 1971).

Beyond the problem of characterizing radiation climates of vegetative stands engendered by the extreme variability of beam radiation in space and time, is the further problem of defining such climates in a biologically meaningful manner. Ramann (1911)

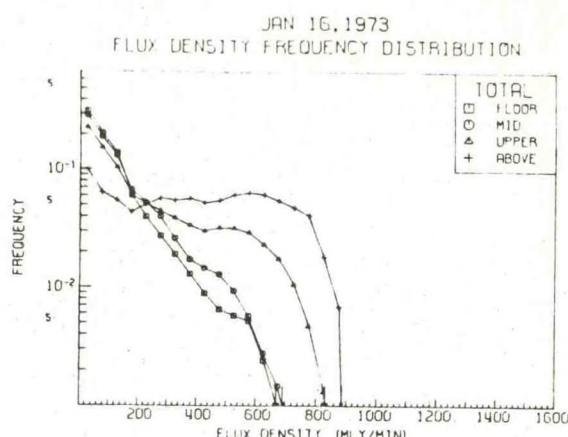


FIG. 7. Smoothed frequency distributions of total radiation flux densities observed within and above the winter leafless forest on a clear midwinter day. Millilangleys $\times 41.84 =$ joules m². ORNL Dwg. 76-15803.

pointed out that the presence of beam radiation in plant stands produces nonnormal frequency distributions of radiant flux densities, thereby making the use of mean values less than satisfactory for many purposes. Mean radiation values are especially poor characterizations of radiation climates in terms of processes such as photosynthesis and transpiration which vary nonlinearly with radiant flux density (Norman et al. 1971).

Typically, radiant flux density frequency distributions are bimodal in the upper reaches of fully leafed plant canopies (Niihiski et al. 1970, Hutchison 1971) and are unimodal and tend to be skewed at greater canopy depths (Ovington and Madgwick 1975, Hutchison 1971, Hutchison and Matt 1973). Using a 50-mly/min [= 2.092 kJ/(m² min)] class interval and a 5-point smoothing procedure to reduce noise, we construct the distributions of Fig. 7 for this winter day. The above-canopy distribution is roughly rectangular while within-forest distributions are unimodal and skewed as previously reported. Modal frequencies at all levels in the forest are in the 0- to 50-mly/min class and the modal frequencies are shown to increase with depth. According to these data, <2% of the radiation received within the winter leafless forest occurs at flux densities exceeding 200 mly/min [= 8.368 kJ/(m² min)] despite incident midday flux densities of the order of 900 mly/min [= 37.656 kJ/(m² min)]. Because of penumbral effects, radiant flux densities in the leafless forest are severely reduced below those incident. Despite the accentuation of the skewness of these distributions effected by the plotting of the ordinate to a log scale, it is evident from Fig. 7 that mean daily radiation values are poor characterizations of leafless forest radiation regimes. Since the kurtosis of these distributions decreases and

JUNE 14, 1972

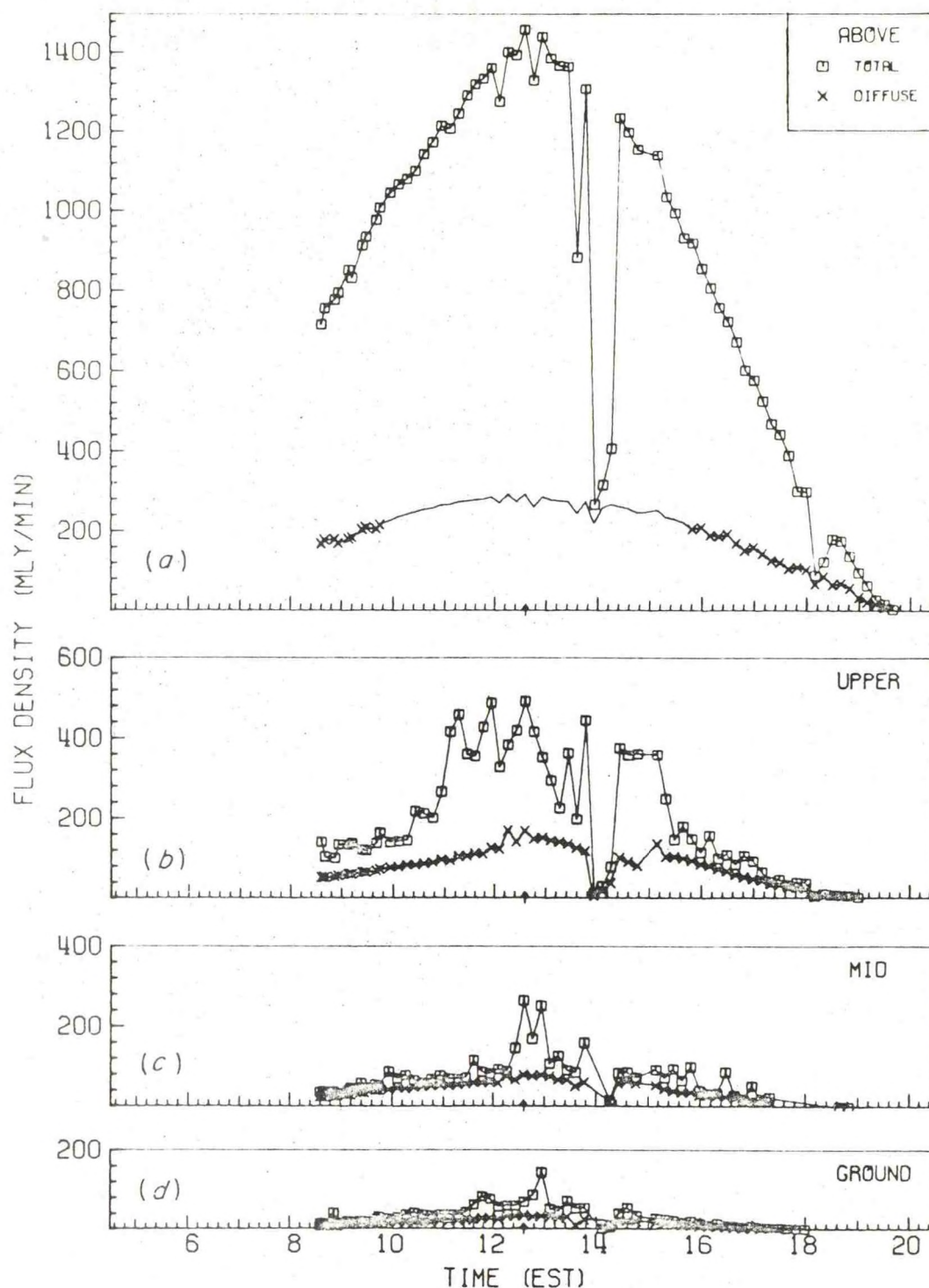
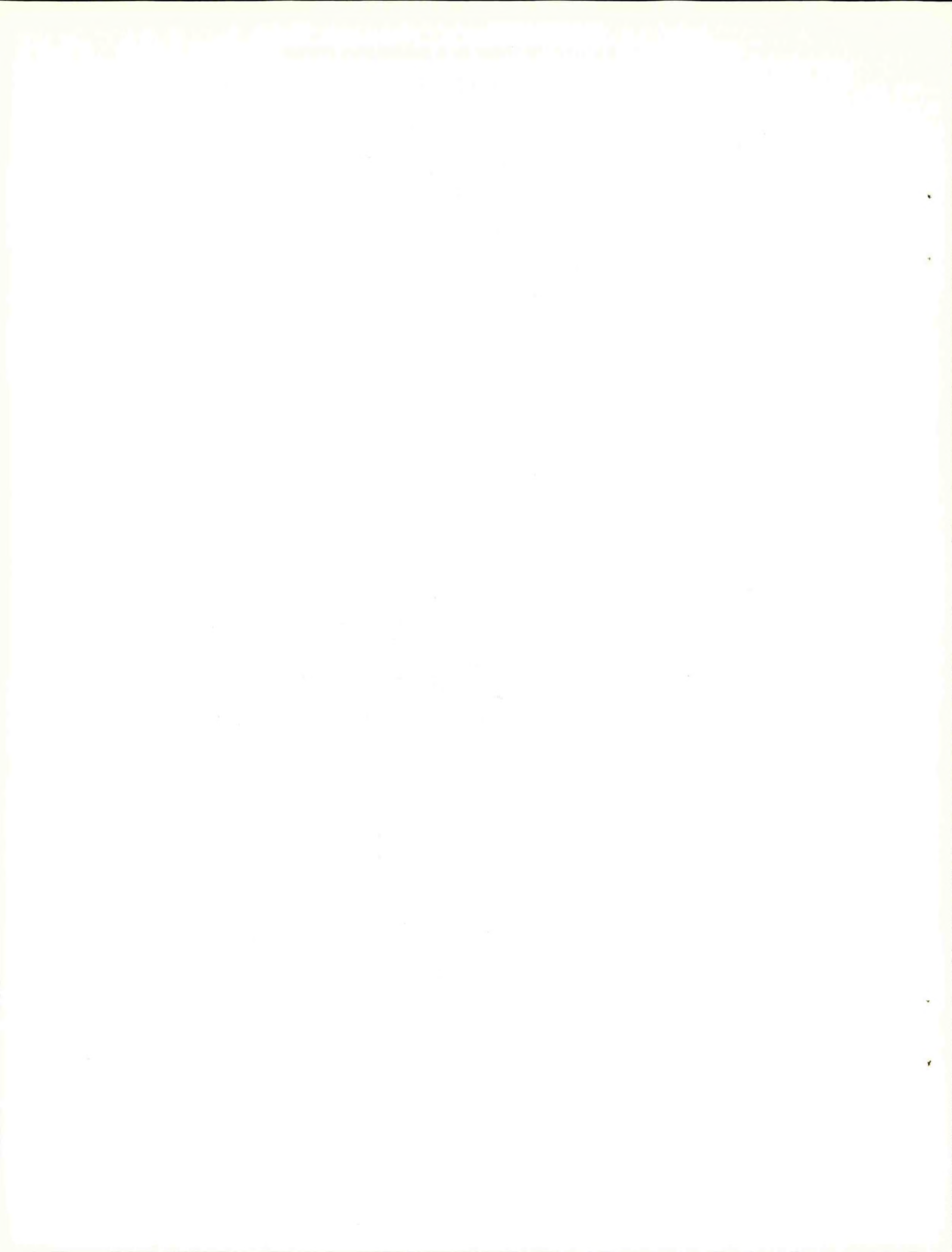


FIG. 8. Diurnal course of average radiation on a mostly clear day in the summer fully leafed forest: (a) above canopy, (b) 16 m, (c) 3 m, and (d) 0 m average total and diffuse radiation records. The portion of the above canopy diffuse radiation curve lacking symbols is estimated. See text for details. Millilangleys $\times 41.84 = \text{joules/m}^2$. ORNL Dwg. 76-16171.



before, the asymmetry of the within-forest curves about solar noon reflects that insufficient measurement replications were made to account for the spatial heterogeneity in structure in this forest.

Views of the fully leafed forest canopy at 0 and 16 m are shown in Figs. 9 and 10. As indicated by these photos, the sky in the region just above the horizon is completely occluded at both levels. At higher angular elevations, more canopy opening is present, but even at 16 m most openings are small and irregularly distributed. Since the distance to which beam radiation can penetrate undiminished through an opening in an opaque surface is a function of the diameter of the opening (Horn 1971), the greatly diminished sizes of canopy openings from winter (Fig. 4) to summer implies greatly decreased beam radiation penetration by virtue of increased penumbral effects (Miller and Norman 1971). Hence, despite the greatly increased amount of beam radiation incident upon the summer forest, greater absorption and attenuation of this radiation is effected by the fully leafed canopy, and the fraction of radiation penetrating the canopy decreases.

Figure 11 emphasizes this reduction. The fractional penetration of total radiation and both its components are reduced from those of winter, especially at midday. Since these midday values for beam and diffuse radiation penetration are suspect by virtue of the use of estimated incident diffuse radiant flux densities, we will not consider them further. However, values for the penetration of total radiation are derived from observed data and should be reasonable. The change in shape of the morning and afternoon portions of the curves of Fig. 11 from those of winter (Fig. 5) are also of interest. Since there is no abrupt change from occluded to unoccluded sky in the fully leafed canopy (Figs. 9 and 10), the fractional penetration of radiation in general and of diffuse radiation in particular increases much more gradually in summer (Fig. 11b) than in winter (Fig. 5b).

Despite the reduction in beam radiation penetration into the fully leafed forest, Fig. 12 shows that midday spatial variabilities are larger at 16 m in summer than in winter (Fig. 6). Variability at 3 m is somewhat decreased while that at the forest floor is strongly reduced. Peak values occur only at midday when significant beam penetration can occur. Earlier and later in the day, space variation is much lower at all three levels. The increased upper canopy space variation with a fully leafed canopy reflects increased heterogeneity in the upper canopy when leaves are present.

As in winter, the summer clear day flux density frequency distributions approach rectangular above and are unimodal and highly skewed within the forest

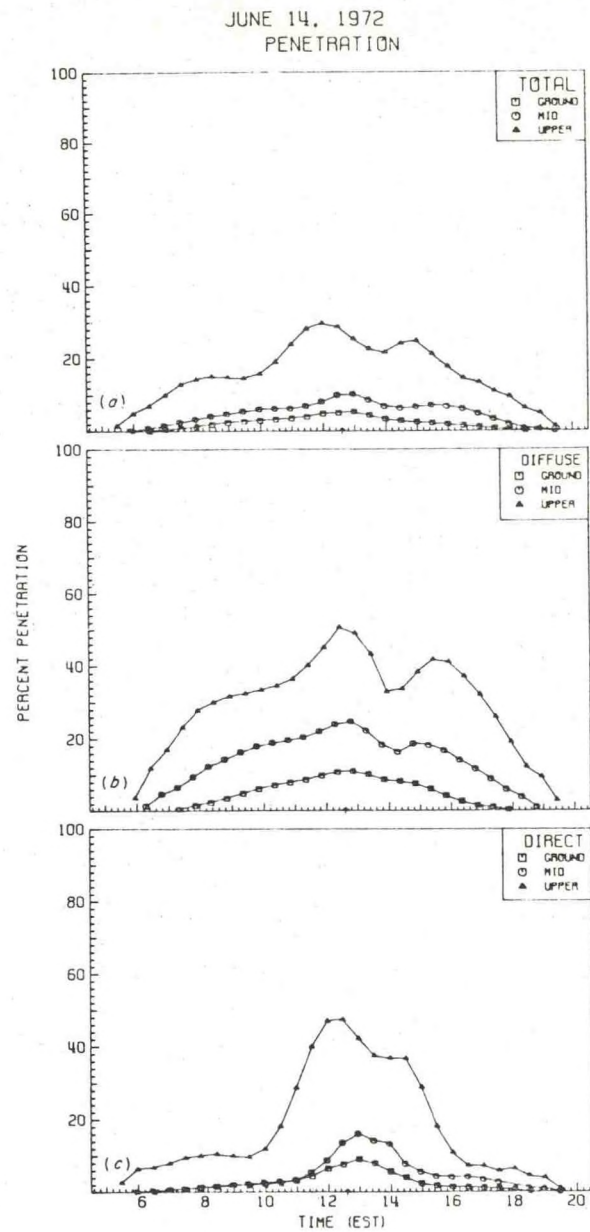


FIG. 11. Smoothed course of average fractional penetration of solar radiation in the summer fully leafed forest under clear skies: (a) total, (b) diffuse, and (c) direct beam radiation. ORNL Dwg. 76-16857.

(Fig. 13). Much higher flux densities are received by the forest in summer by virtue of the greatly increased midday solar elevations. Nevertheless, the incidence of radiation at flux densities $>200 \text{ mly/min}$ are decreased at the lower levels in the summer forest because of the increased penumbral overlap in the sunflecks formed by the much smaller canopy openings (Figs. 7 and 13). At 16 m, incidence of higher flux density sunflecks increases somewhat (since the incident diffuse is estimated to peak at around 200

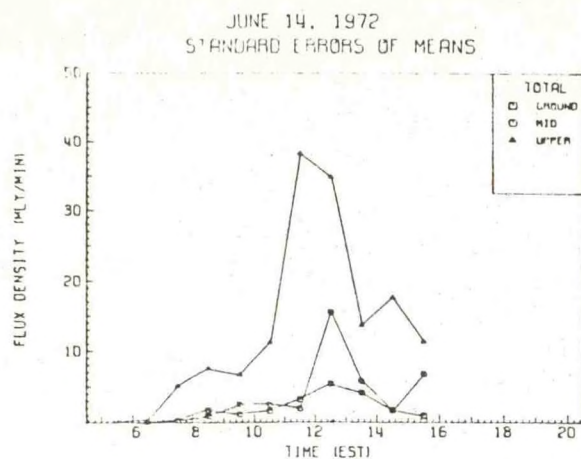


FIG. 12. Smoothed course of spatial variability of total radiation received within the summer fully leafed forest as measured by the half-hour time averaged instantaneous standard error of the space mean total radiation. Millilangleys $\times 41.84 = \text{J/m}^2$. ORNL Dwg. 76-15795.

mly min at midday on 14 June, all flux densities in excess of this amount probably stem from beam radiation) but still drops to insignificant frequencies at rather low flux densities compared to those incident upon the forest. Essentially no radiation reaches 0 or 3 m at flux densities > 200 mly/min, while only about half of that received at 16 m exceeds this flux density.

To give biological perspective for these data, Dinger (1971) has reported that light saturation in *Liriodendron tulipifera* occurs at flux densities of about 400 mly/min [$= 16.736 \text{ kJ}/(\text{m}^2 \text{ min})$], while the compensation point for this intolerant species occurs at about 40 mly/min [$\approx 1.674 \text{ kJ}/(\text{m}^2 \text{ min})$]. Hence, despite the great attenuation of radiation and the severe reduction of incidence of higher flux density radiation by the fully leafed forest, few leaves in this forest received insufficient quantities of radiation for photosynthetic compensation on clear summer days. However, since leaves transmit green and near infrared wavelengths preferentially, much of the radiation present within the summer forest may be photosynthetically inactive.

Overcast day forest radiation regimes

With overcast skies, amounts of radiation reaching the surface of the earth or of a plant community are reduced from those present on clear days because of absorption and back-reflection of radiation by and from the cloud cover. Furthermore, direct beam radiation is diffused by the process of transmission through clouds, and consequently that radiation incident upon a forest on overcast days is nearly entirely diffuse. This is evident in Fig. 14a.

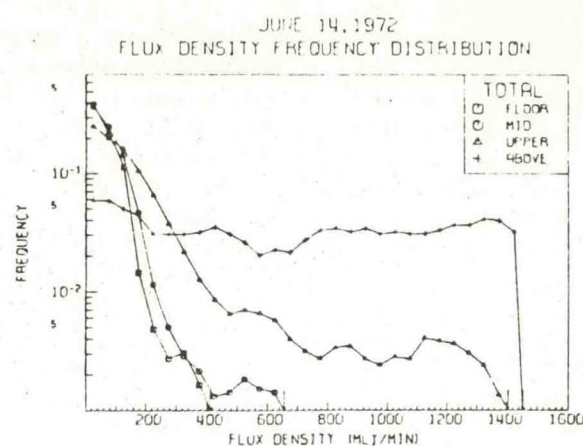


FIG. 13. Smoothed frequency distributions of total radiation flux densities within and above the summer fully leafed forest on a mostly clear summer day. Millilangleys $\times 41.84 = \text{J/m}^2$. ORNL Dwg. 76-15796.

Throughout the morning and early afternoon of this January day, skies were heavily overcast; total and diffuse flux densities are nearly equal. That difference that is present is most likely the result of the presence of the shadow band since our diffuse values are uncorrected for radiation stemming from the portion of the sky occluded by the band. In midafternoon the sky cleared partially, resulting in a sharp rise in incident total radiation.

During the overcast portion of this day, the records of total radiation above and within the leafless forest of Fig. 14 are quite similar to the equivalent diffuse records on the clear day of 16 January (see Fig. 3). Total radiation within the forest on the overcast day exceeds the amount of diffuse radiation received there on the clear January day because of the greater amounts of diffuse radiation incident on the forest on the overcast day. Otherwise the diurnal trends are similar.

Comparison of Figs. 15 and 5a for the overcast and clear winter days, respectively, shows that more of the incident radiation penetrates the forest on the overcast day than on the clear day. However, comparison of Fig. 15 with Fig. 5b shows that the proportion of radiation from overcast skies that penetrates the forest is less than that of the diffuse that penetrates on a clear day. This indicates that the enrichment of diffuse radiation within the forest on clear days by down-reflected direct beam radiation may be significant even in the leafless winter forest.

Because of the absence of direct beam radiation, the forest is much more uniformly illuminated on this overcast day. The space variation in total radiation is around ± 1 mly/min [$\approx 41.8 \text{ J} \cdot \text{m}^{-2} \cdot \text{min}^{-1}$] or less at all levels in the forest. With the clearing skies in midafternoon, the space variation

JANUARY 30, 1973

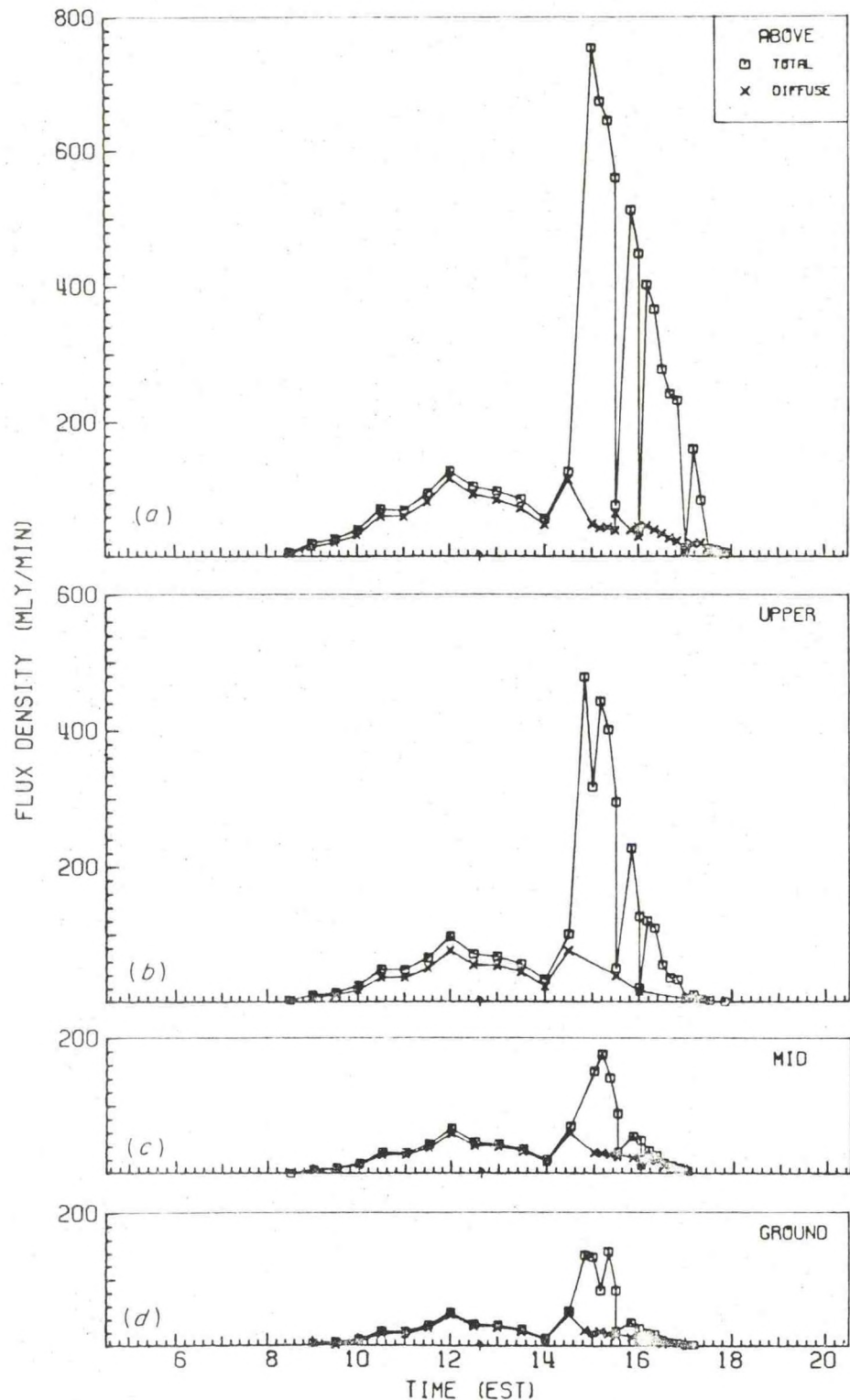


FIG. 14. Diurnal course of average radiation on an overcast day in the winter leafless forest: (a) above canopy, (b) 16 m, (c) 3 m, and (d) 0 m. Millilangleys $\times 41.84 = \text{J/m}^2$. ORNL Dwg. 76-15808.

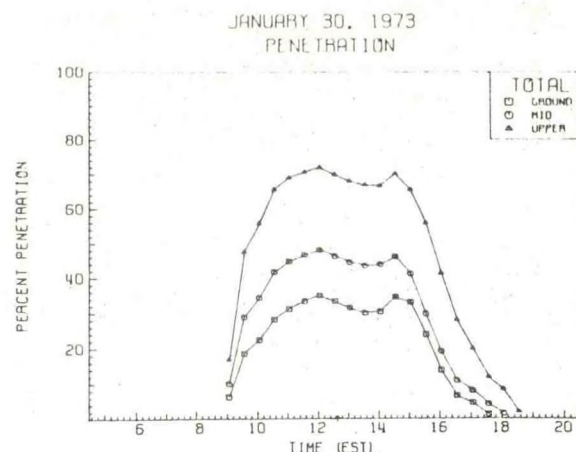


FIG. 15. Smoothed daily course of average fractional penetration of solar radiation from an overcast sky in the winter leafless forest. ORNL Dwg. 76-16784.

rises dramatically to values comparable to those of the clear winter day shown in Fig. 6.

As shown on Fig. 16, no radiation was incident on the forest at flux densities $>900 \text{ mly/min}$. Within the forest, the woody biomass is shown to effect considerable change in the frequency distributions of radiant flux densities from that incident. Only at the 16-m level are there significant amounts of radiation present at flux densities exceeding 200 mly/min.

Radiation received within and above the summer fully leafed forest on a heavily overcast day is shown in Fig. 17. The irregularity of these curves indicates that the density of the cloud cover on this June day was not as uniform in time as on the overcast January day. Nevertheless, the density of cloud cover was sufficiently high to reduce incident direct beam flux densities to very low values.

As would be expected with reduced insolation, the radiation within the forest is much reduced from that received on the clear day of 14 June (see Figs. 8 and 17). Almost no radiation penetrates to the 3- or 0-m levels. The amounts of diffuse radiation penetrating the forest shown in Figs. 17c and d are substantially reduced from those penetrating the forest on the clear June day of Figs. 8b and c despite comparable magnitudes of incident diffuse radiation on these two days. This further illustrates the importance of direct beam enrichment of diffuse radiation within the forest through transmission and down-reflection processes.

Comparison of the winter and summer overcast day penetration of Figs. 15 and 18 shows that the fully leafed forest canopy effects a considerable reduction in the penetration of diffuse radiation from overcast skies. Furthermore, whereas in winter the proportion of radiation penetrating the forest is in-

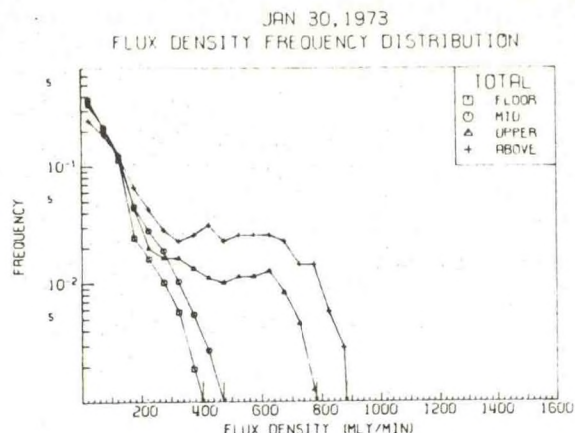


FIG. 16 Smoothed frequency distributions of total radiant flux densities observed within and above the winter leafless forest on an overcast day. Millilangleys $\times 41.84 = \text{J/m}^2$. ORNL Dwg. 76-15801.

creased with overcast skies, the reverse is true in the summer leafed forest. Comparison of Figs. 18 and 11a shows that the fraction of total incident radiation penetrating to all forest levels is reduced by the cloud cover when the forest is fully leafed. This finding is in disagreement with results of studies by Brecheen (1951) and by Tsel'Niker (1968). As Anderson (1964a) has pointed out, forests in general show decreasing canopy density from the horizon to the zenith. This is especially true in conifer forests and is increasingly true of deciduous forests at higher latitudes. Since uniformly overcast skies usually have brightness distributions that increase from horizon to zenith (Moon and Spencer 1942), in contrast to clear skies where the brightest area of the sky is immediately adjacent to the solar disk (Dorno 1919, Kimball and Hand 1921, Pokrowski 1929), a forest whose canopy density decreases toward the zenith will admit a greater proportion of incident radiation on overcast days than on clear days. As the canopy photograph of our forest in winter shows (Fig. 4), the leafless forest does have minimal canopy density at the zenith and the penetration of radiation into the forest in this phenologic phase agrees with results reported in the literature. However, measurements of canopy opening distributions on replicated canopy photos from this forest in full leaf indicate maximum sky area visible at midelevation angles (Fig. 19). Hence, our results for the summer overcast day are in disagreement with those of Brecheen (1951) who worked in western conifer forests and of Tsel'Niker (1968) who studied radiation in an oak forest near Moscow.

Comparison of clear day diffuse radiation (Figs. 8b,c, and d) with overcast day total (Figs. 17b,c, and d) shows that more diffuse radiation is received

JUNE 20, 1972

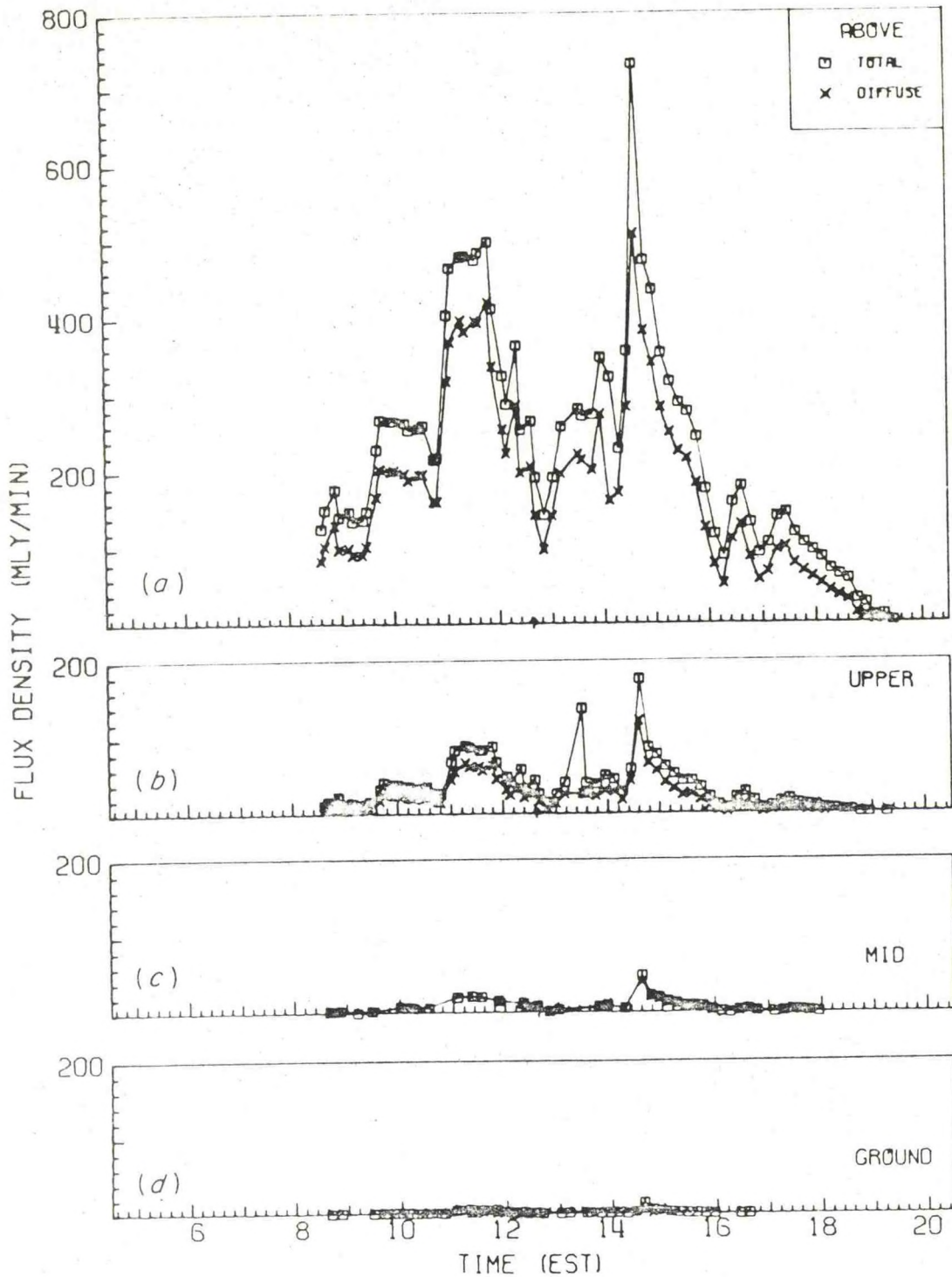


FIG. 17. Diurnal course of average radiation on an overcast day within and above the summer fully leafed forest: (a) above canopy, (b) 16 m, (c) 3 m, and (d) 0 m. While the detail of the radiation records at 3 and 0 m is lost when plotted to this scale, the reduction of radiant flux densities to very low levels is obvious. Mililangleys $\times 41.84 = \text{J/m}^2$. ORNL Dwg. 76-15809.

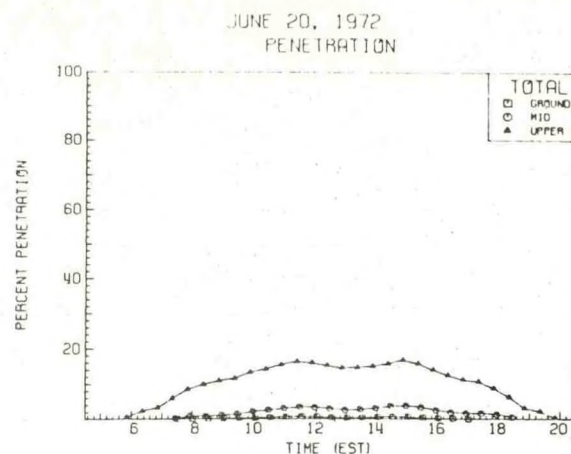


FIG. 18. Smoothed daily course of average fractional penetration of solar radiation from an overcast sky in the summer fully leafed forest. ORNL Dwg. 76-16783.

within the fully leafed forest on a clear day than total radiation on this overcast day. On clear days, significant enrichment of diffuse radiation within the forest occurs because of the down-reflection and

transmission of direct beam radiation from and through leaf tissues, which has the effect of increasing the apparent proportion of incident diffuse radiation that penetrates the canopy (Hutchison and Matt 1976). Thus, in the fully leafed forest, fractional clear day diffuse penetration and absolute quantities of diffuse radiation exceed overcast day fractional radiation penetration and amounts.

As in the winter leafless forest, overcast day illumination within the summer fully leafed forest is quite uniform in space and in time. Variabilities at the lower levels are $< \pm 1$ mly/min throughout the overcast day. In the upper canopy (16 m), this variation ranges from ± 1 to ± 5 mly/min. The cloud cover effects a considerable reduction in spatial and temporal variability in radiation through its elimination of the direct beam component.

Because of the lack of high flux density radiation incident upon the forest on this day (Fig. 20), skewness in the flux density distributions within the forest practically disappears. Modal frequencies in the 0- to 20-mly/min flux density class are increased and the frequencies drop to insignificant values at quite low flux densities at all levels in the forest.

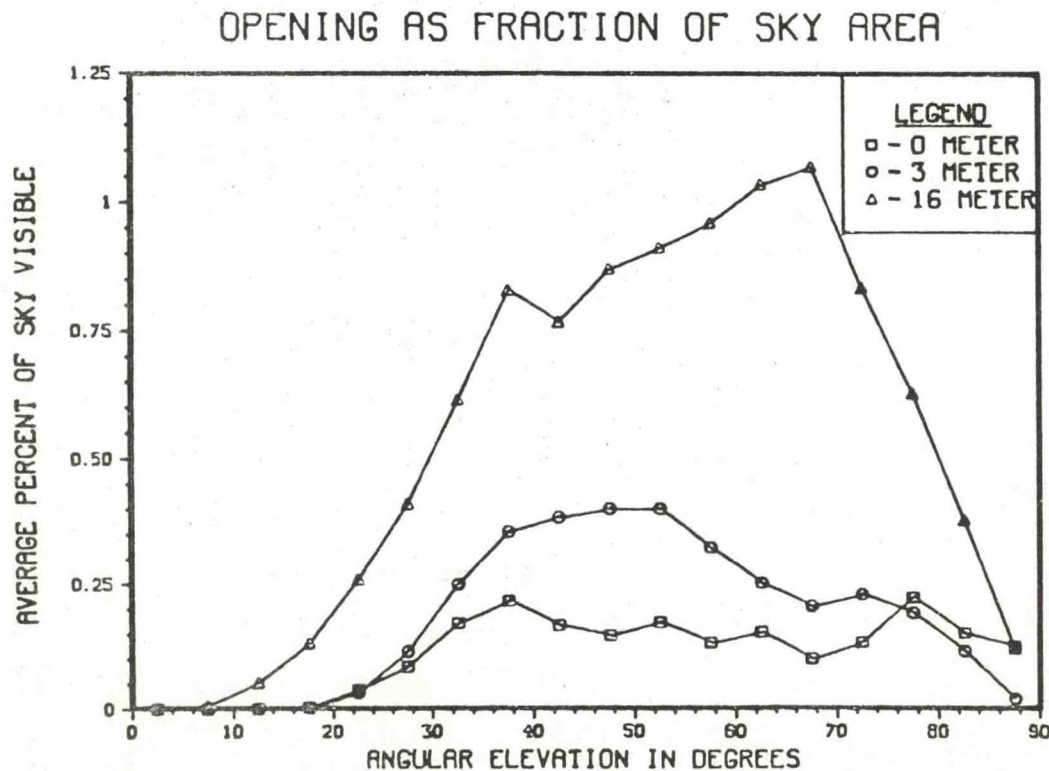


FIG. 19. Distribution of canopy opening expressed as a percent of the total projected area of sky over angular elevation. ORNL Dwg 77-9655.

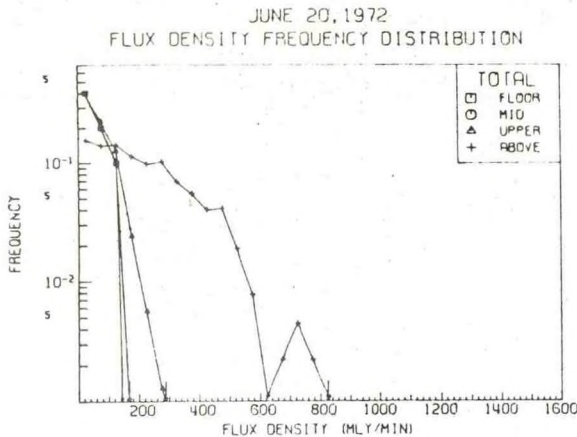


FIG. 20. Smoothed frequency distributions of total radiant flux densities observed within and above the summer fully leafed forest on an overcast day. Millilangleys $\times 41.84 = \text{J/m}^2$. ORNL Dwg. 76-15799.

Phenoseasonal variation in forest radiation regimes

Figure 21 shows the daily radiative component totals for a clear day in each of the seven phenoseasons defined in Fig. 2 as well as for the two overcast days presented above. As shown, the phenoseasonal course of incident total radiation on the clear days departs considerably from the sinusoidal seasonal variation of potential incident radiation. As would be expected, the minimum total radiation incident on the forest occurs on the winter day, but because of increasing atmospheric turbidity through spring and into summer, the annual observed maximum occurs during the summer leafing forest phenoseason rather than during the summer fully leafed forest phenoseason nearer the summer solstice.

Incident diffuse radiation is minimal during the winter season and slowly increases through the spring. In summer, the incident diffuse radiation increases substantially as a result of increased atmospheric turbidity, then declines again in autumn. Minimum direct beam radiation reaches the forest in winter, while maximum daily totals of incident direct beam are observed in the spring leafing forest phenoseason. After this phenoseason, the direct beam totals are reduced somewhat, despite the high daily totals of radiation incident on the forest because of the increases in incident diffuse radiation.

The daily totals of incident radiation on heavily overcast days are much reduced from those of the clear days and approach the daily totals of clear day diffuse (denoted by stars on Fig. 21). Although the total for the summer overcast day exceeds that of the winter day as would be expected, we have no measures of the relative densities of the cloud cover on these days and hence, this is merely fortuitous.

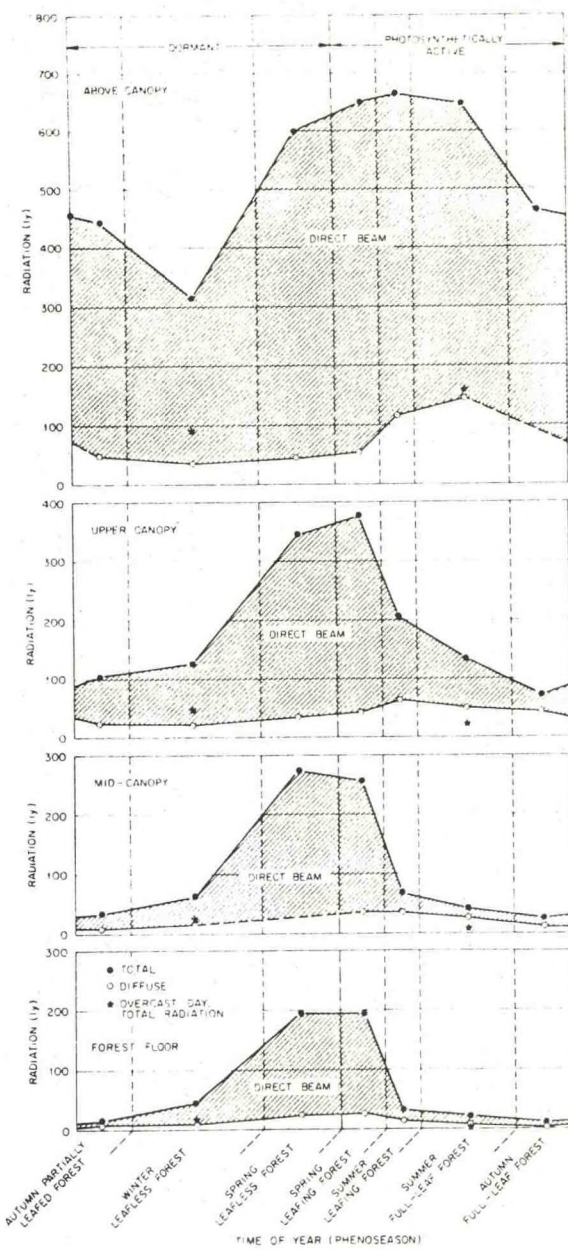


FIG. 21. Annual clear day radiation regimes in and above the *Liriodendron* forest. Starred values are overcast day totals for each of these levels. To convert langley (ly) to joules per square metre (J/m^2), multiply by 4.184×10^4 . ORNL Dwg. 75-1134.

Within the canopy, the seasonal course of total radiation received closely follows that of the radiation incident upon the forest during the winter and early spring. With leaf expansion however, the radiation regimes within the forest change abruptly. Daily total radiation received at the lower two forest levels begins to decrease in the spring leafing phenoseason, while in the upper canopy a continued increase is

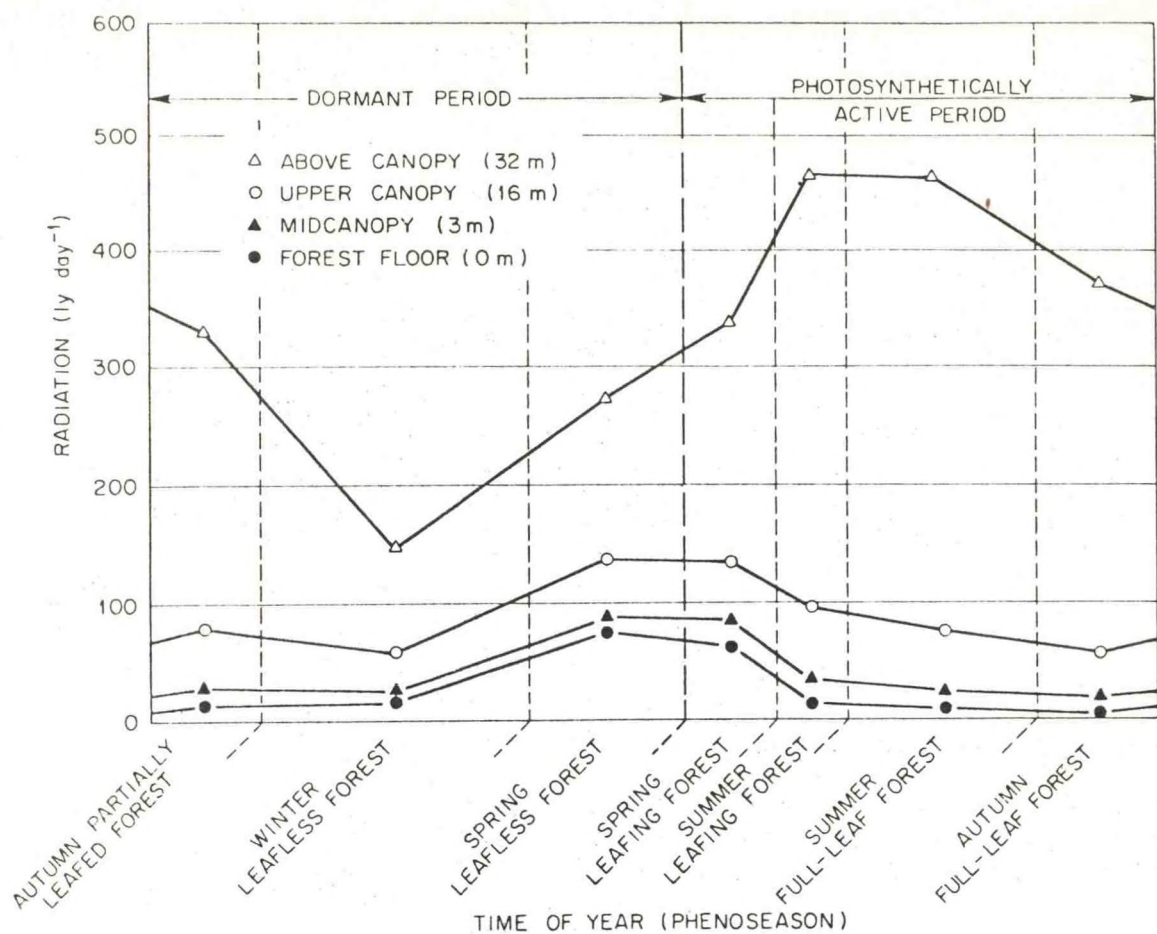


FIG. 22. Approximation of the annual regimes of daily total radiation in and above the *Liriodendron* forest. Langley $\times 4.184 \times 10^4 = \text{J/m}^2$. ORNL Dwg. 75-1133R.

evident. With continued leaf expansion, daily totals drop sharply at all levels in the forest during the summer leafing forest phenoseason despite increasing totals of radiation incident upon the forest. Throughout the summer and early autumn, daily total radiation received within the forest continues to decrease as a result of decreasing incident radiation and lower solar elevations throughout the day. Then with abscission in late autumn, radiation in the forest again increases despite the continued decrease in above-canopy isolation.

Daily totals of diffuse radiation received within the forest on clear days show much less seasonal variation than daily totals of either total or direct beam radiation. Maximum daily totals of diffuse radiation occur in the early summer in the upper canopy and in spring at the lower levels. Minimum diffuse radiation values occur in the autumn fully leafed forest phenoseason at the forest floor, in the autumn partially leafed forest phenoseason at midcanopy, and in winter in the upper canopy. Direct beam radiation

in the forest is maximal through the early spring and minimal in summer and early autumn.

Overcast day totals are reduced in the winter forest and are strongly reduced in the summer fully leafed forest. Because of the leaf cover, overcast summer day totals of radiation in the forest are less than those in the winter leafless forest despite the greater daily total radiation incident upon the forest on the summer overcast day.

While the clear day radiation totals indicate the interactions of changing earth-sun geometry and forest phenology throughout a year, they cannot serve as an approximation of the annual radiation regime in or above the forest because most days are not clear. Using the techniques outlined in the methods section above, we have approximated an annual radiation regime (Fig. 22) in and above this forest using the discontinuous observations of radiation in this forest and the continuous record of solar radiation collected in Oak Ridge, approximately 10 km to the north. The daily totals shown on this figure follow

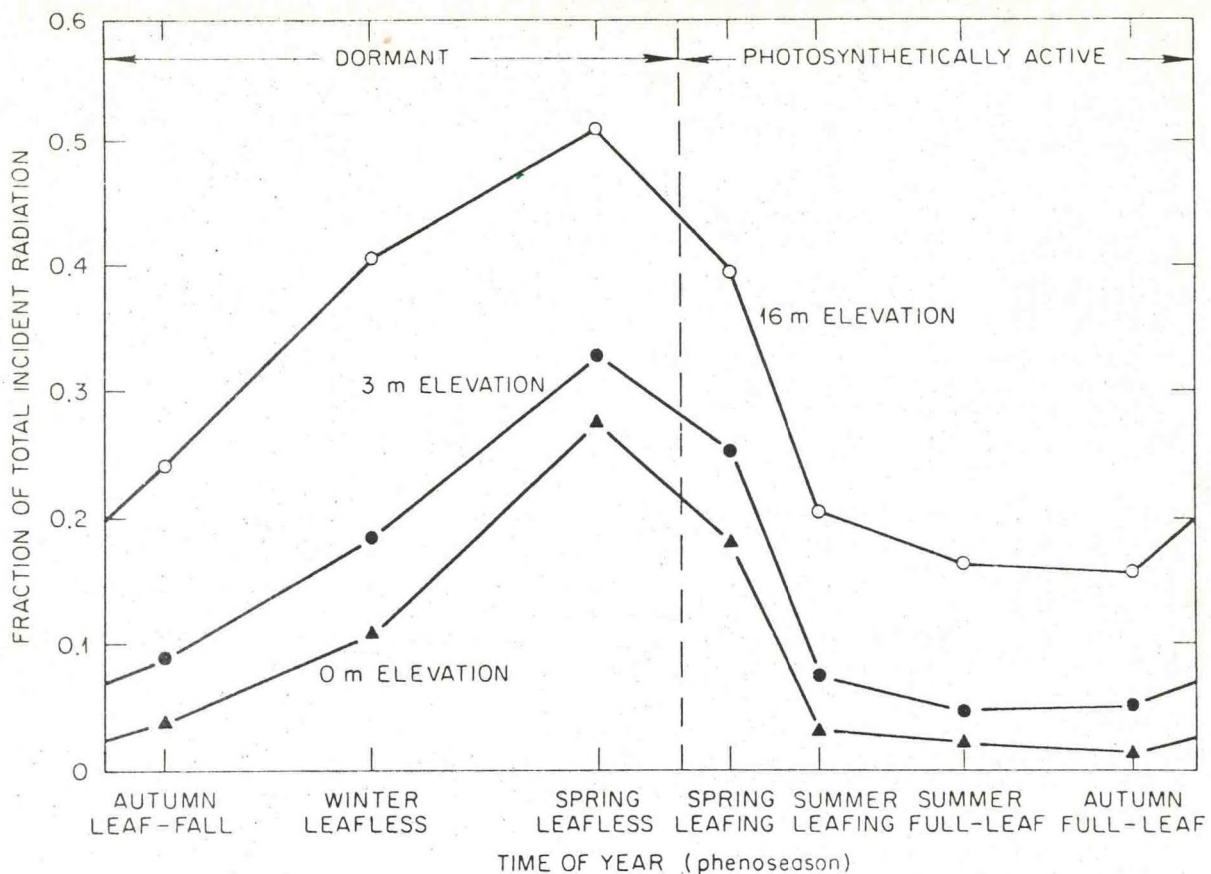


FIG. 23. Derived annual course of average daily fractional penetration in the *Liriodendron* forest. ORNL Dwg. 74-11563.

closely the trends of the clear day data of Fig. 21, but the absolute values are much reduced at all levels in and above the forest. Unlike the clear day totals, maximum average daily totals occur at all levels in the forest during the spring leafless forest phenoseason. The minimum daily totals at all levels occur during the autumn fully leafed forest phenoseason.

Normalizing these daily totals within the forest by that incident upon the forest yields Fig. 23, the annual course of average daily penetration of total radiation in the forest. The interaction between forest phenology and earth-sun geometry is clearly shown on this figure. With increasing solar elevations in the spring, penetration rates increase at all levels in the forest. With the advent of leaf expansion in early April, the penetration rates begin to decline. Then with the stabilization of leaf area, the penetration rates continue to decline, but at very low rates as a result of decreasing solar elevations after the summer solstice. Finally, with leaf abscission in the autumn, these penetration rates again begin to rise as a result of decreased canopy density despite the continued decrease in solar elevations.

From these same data, we approximate the annual incoming radiation budget for this forest in Table 2. Although insolat on the forest during the photosynthetically active portion of the year is over one and one-half times as great as that during the inactive period, less radiation is received within the forest at all levels than in the leafless period because of the presence of leaves. The greatest fraction of the total radiation received within the forest at all levels is received during the spring leafless forest phenoseason. Furthermore, the fraction of the yearly total radiation received during this phenoseason increases with depth to about 45% at the forest floor. Following this phenoseason, these fractions decrease to much lower values in the fully leafed forest phenoseasons. Because of this, the development of the forest floor vegetation peaks during the spring and mostly ceases by summer. Most of the herbaceous plants in this forest complete their annual cycle of growth and reproduction in the spring leafless and leafing forest phenoseasons.

Assuming an exponential attenuation of radiation with depth in the forest and utilizing our knowledge

TABLE 2. Approximation of radiation received within the *Liriodendron* forest throughout the year. To convert langleyes (ly) to joules per square metre (J/m^2), multiply by 4.184×10^4

| Phenoseason | Duration (days) | Total radiation received (langleyes [percent of yearly total]) | | | |
|--|--------------------|--|-----------------------------|-------------------------|----------------------------|
| | | Above (32 m) % | Upper canopy (16 m) % | Midcanopy (3 m) % | Forest floor (0 m) % |
| Winter leafless | 91 | 13,300 (11.5%) | 5,400 (17.5%) | 2,400 (16.9%) | 1,500 (16.5%) |
| Spring leafless | 55 | 15,000 (13.0%) | 7,600 (24.6%) | 4,900 (34.5%) | 4,100 (45.0%) |
| Spring leafing | 30 | 10,200 (8.8%) | 4,000 (12.9%) | 2,500 (17.6%) | 1,800 (19.8%) |
| Summer leafing | 26 | 11,700 (10.1%) | 2,400 (7.8%) | 800 (5.6%) | 300 (3.3%) |
| Summer full-leaf | 67 | 31,500 (27.2%) | 5,100 (16.5%) | 1,500 (10.6%) | 700 (7.7%) |
| Autumn full-leaf | 57 | 21,100 (18.2%) | 3,300 (10.7%) | 1,000 (7.0%) | 200 (2.2%) |
| Autumn partial-leaf | 39 | 12,900 (11.2%) | 3,100 (10.0%) | 1,100 (7.8%) | 500 (5.5%) |
| Photosynthetically active period total | | 74,500 (64.4%) | 14,800 (47.9%) | 5,800 (40.8%) | 3,000 (33.0%) |
| Dormant period total | | 41,200 (35.6%) | 16,100 (52.1%) | 8,400 (59.2%) | 6,100 (67.0%) |
| Yearly total | | 115,700 | 30,900 | 14,200 | 9,100 |

of the seasonal and phenological changes occurring, we synthesize these data on the seasonal variation in forest radiation climates in Fig. 24. This figure represents our estimates then, of the annual cycle of radiation regimes in this forest. The penetration of greater amounts of radiation into the leafless forest as solar elevations increase from winter to spring is shown by the height depression of radiation isopleths in spring. With the onset of leaf expansion, this increase is reversed and the isopleths move higher in the forest. After the summer solstice forest structure remains relatively static, and solar elevations slowly decline. With this decline the radiation within the forest declines to the autumn minimum. With leaf abscission in the autumn, radiation isopleths again move slightly deeper into the forest indicating slight increases in radiation received there. With the continued decline in solar elevation after leaf fall is complete, this trend quickly reverses and radiation within the leafless forest declines slightly.

SUMMARY AND CONCLUSIONS

The average amount of radiation received at any time within the forest varies directly as the amount of radiation incident at that time. This holds for total radiation and for its direct beam and diffuse components at all times of the year. Only the proportionalities change in time with varying cloudiness, with changing solar elevations, and with phenological changes in forest structure.

Of the two radiative components, direct beam radiation suffers the greatest attenuation by the forest biomass. The penetration of this component is strongly controlled by the interaction of solar elevation and canopy density variation with angular elevation. The greatest attenuation of direct beam radiation occurs in the overstory canopy in all phenoseasons with decreasing attenuation in lower forest strata.

The diffuse component, on the other hand, is less attenuated by the forest biomass and its attenuation is more uniform in the three-canopy strata of the leafless forest than that of the direct beam component. In the fully leafed forest, the greatest amount of attenuation of diffuse radiation occurs in the overstory canopy as well. Because of the differences in the origin of these two radiative components and the structure of the forest, the diffuse component is attenuated less than direct beam radiation in all seasons and phenological phases of the forest.

With the expansion of leaves in spring, attenuation of both direct beam and diffuse radiation increases. Early in the leafing phase, increasing amounts of these components incident on the forest and rising solar elevations offset the increased attenuation by new leaves in the canopy, and absolute quantities of radiation in the forest continue to increase. With continuing leaf expansion, however, attenuation increases and radiation in the forest decreases. After the forest attains full leaf, both diffuse and direct beam radiation continue to decrease within the forest, despite unchanging forest structure. In the overstory canopy, the decrease in direct beam radiation is much greater than the decrease in diffuse as a result of the increasing optical path lengths of direct beam radiation in the forest with the decreasing solar elevations of late summer and early autumn. The decrease in diffuse radiation in the forest results from the decreasing amounts of incident diffuse radiation with time after the summer solstice.

The variability of radiation in horizontal space in the forest is largely the result of the penetration of direct beam radiation. Hence, the degree of spatial variability varies directly as the amounts of direct beam radiation penetrating the forest canopy throughout the year. Because of the apparent movement of the sun across the sky each day, the sunflecks resulting from the penetration of direct beam radiation

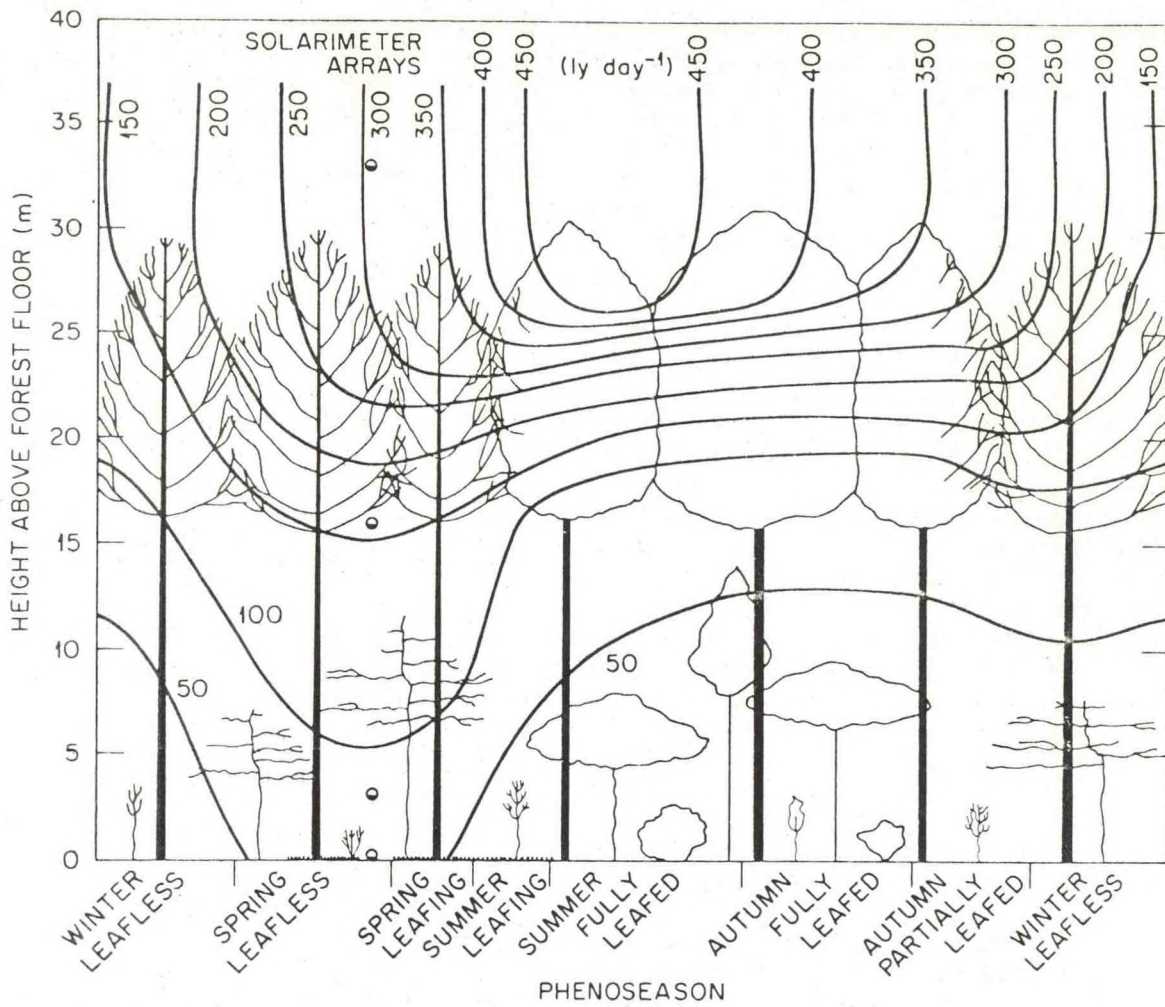


FIG. 24. Synthesized annual course of average daily total solar radiation received within and above a tulip poplar forest. Langley's $\times 4.184 \times 10^4 = \text{J/m}^2$. ORNL Dwg. 76-7581.

move across surfaces in the forest, introducing temporal variation as well. Thus, a direct relationship exists between direct beam radiation penetration and temporal variation in daily forest radiation regimes.

Variation in both space and time decreases with depth in the forest. Space variation in the upper canopy greatly exceeds the $\pm 10\text{-mly/min}$ [$\approx 418 \text{ J} \cdot \text{m}^{-2} \cdot \text{min}^{-1}$] accuracy desirable for energy budget considerations. This implies that more than 12 replications of measurements would be needed in all phenoseasons in the upper canopy to attain this level of precision. Even at the forest floor in the summer fully leafed forest where variation of radiation in horizontal space is generally quite low, our 12 replicated measurements yield variabilities in excess of this level around solar noon. Thus, numbers of replications of measurements needed to attain specific levels of precision vary in vertical space and through time.

In winter, the proportion of radiation penetrating the forest is increased with cloud cover, although absolute values decrease because of lower amounts of incident radiation. Despite the increased penetration of radiation from overcast skies, clear winter day diffuse penetration exceeds that of overcast winter days, indicating that the enrichment of diffuse radiation by reflected direct beam radiation is significant in the winter forest, or that differences in sky brightness distributions between clear and cloudy days effect significant differences in amounts of diffuse radiation penetrating the forest. In summer, the proportion of incident radiation penetrating the forest decreases with increasing cloudiness in contrast to results from other studies reported in the literature. We attribute this difference to a rather different forest structure than has been studied in the past. Our mesic, lower latitude, temperate, deciduous forest, when fully leafed, has greatest amounts of opening at

midelevation angles rather than at the zenith. As far as we are able to determine, the previously studied forests had minimal density at the zenith which interacts with overcast sky brightness distributions to allow greater penetration of radiation on overcast days.

As in winter, the summer overcast day penetration rates of total radiation are substantially less than those of the summer clear day diffuse radiation, indicating again the importance of direct beam enrichment of diffuse radiation in the forest on clear to partly cloudy days.

The amount of direct beam radiation that penetrates the forest strongly controls the distribution of radiant flux densities in space and in time within the forest. Maximum amounts of direct beam radiation penetrate this forest in the early spring and, as a result, a substantial portion of the radiation received in the forest arrives at high flux densities. As the leaves expand later in the spring and in early summer, the penetration of direct beam radiation is severely reduced within the forest. This in turn causes a major reduction in the amount of higher flux density radiation within the forest. After the forest attains full leaf, very little radiation is present at any level in the forest at flux densities exceeding 200 mly/min, despite incident flux densities as high as 1,500 mly/min [$= 62.76 \text{ kJ} \cdot \text{m}^{-2} \cdot \text{min}^{-1}$]. With decreasing solar elevations after the summer solstice, further reductions in the penetration of high flux density radiation occur. Then with leaf abscission, slight increases in direct beam penetration effect the penetration of radiation at higher flux densities once again. With the decreasing solar elevations of autumn and early winter, these increases are soon eliminated and the amount of high flux density radiation within the forest decreases from autumn to winter.

Greatest amounts of radiation are received within the forest in the spring before leaf expansion begins. The least radiation is received with the lower solar elevations and shorter day lengths of early autumn while the forest is still fully leafed. With leaf fall later in the autumn, radiation in the forest increases slightly but then decreases again with the winter decline of insolation.

ACKNOWLEDGMENTS

The collection and analyses of these data were greatly aided by the assistance of Mike Breed, Mark Hanon, and Vada Maxey, Oak Ridge Associated Universities Summer Trainees; Karen Jamrusz and Barbara Rooney, Work-Study Program, University of Tennessee; and Eugene Culver and Jerry Sharp, ATDL. Computer programming for data display by R. T. McMillen, ATDL is hereby acknowledged. Reviews by W. T. Hinds, Battelle Northwest Laboratories, Hanford Reactor Site, Richland, Washington; C. E. Murphy, Jr., Environmental Transport Division, Savannah River Laboratory, Aiken, South Carolina; and S. B. McLaughlin and R. S. Strand, En-

vironmental Sciences Division, ORNL, resulted in significant improvements in this paper. Comments and criticisms of the anonymous Ecological Society referees were of great benefit to the authors and resulted in increased clarity and readability of this report.

This research supported in part by the Eastern Deciduous Forest Biome, US-IBP, funded by the National Science Foundation under Interagency Agreement AG-199, BMS 76-00761 with the U.S. Energy Research and Development Agency, Oak Ridge National Laboratory and in part by the Division of Biomedical and Environmental Research, ERDA, Contribution No. 290, Eastern Deciduous Forest Biome, US-IBP, ATDL Contribution No. 75/18.

LITERATURE CITED

- Anderson, M. C. 1964a. Studies of the woodland light climate. I. The photographic computation of light conditions. *J. Ecology* 52:27-41.
- . 1964b. Studies of the woodland light climate II. Seasonal variation in light climate. *J. Ecology* 52: 643-663.
- . 1964c. Light relations of terrestrial plant communities and their measurements. *Biol. Rev.* 39:425-486.
- Anderson, M. C., and O. T. Denmead. 1969. Short wave radiation on inclined surfaces in model plant communities. *Agron. J.* 61:867-872.
- Brecheen, K. G. 1951. Transmission of shortwave radiation through forest canopy. *Coop. Snow Invest., Corps of Eng., U.S. Army Res. Note SPDGC* 627-51, 18 p.
- Dinger, B. E. 1971. Net photosynthesis and production of *Liriodendron tulipifera* as estimated from carbon dioxide exchange. US-IBP Eastern Deciduous Forest Biome Memo Rpt. No. 71-75, 8 p.
- Dinger, B. E., C. J. Richardson, and R. K. McConathy. 1972. Dynamics of canopy leaf area development and chlorophyll phenology in yellow poplar. US-IBP Eastern Deciduous Forest Biome Memo Rpt. No. 72-164, 15 p.
- Dorno, C. 1919. *Physik der Sonnen-und Himmelstrahlung*. Vieweg, Braunschweig, Germany.
- Drummond, A. J. 1956. On the measurement of sky radiation. *Arch. Meteorol. Geophys. Bioklimatol. Ser. B*, 7:413-436.
- Fritz, S. 1958. Transmission of solar energy through the earth's clear and cloudy atmosphere, p. 17-36. In E. F. Carpenter [ed.] Trans. of the conf. on the use of solar energy: The scientific basis. Univ. Ariz. Press, Tucson, Vol. 1.
- Gay, L. W., K. R. Knoerr, and M. O. Braaten. 1971. Solar radiation variability in the floor of a pine plantation. *Agric. Meteorol.* 3:39-50.
- Horn, H. W. 1971. The adaptive geometry of trees. Princeton Univ. Press, Princeton, N.J., 144 p.
- Horowitz, J. L. 1969. An easily constructed shadow-band for separating direct and diffuse radiation. *Solar Energy* 12:543-545.
- Hutchison, B. A. 1971. Spatial and temporal variation in the distribution and partitioning of solar energy in a deciduous forest ecosystem. US-IBP Eastern Deciduous Forest Biome Memo Rpt. No. 71-82, 40 p.
- Hutchison, B. A., and D. R. Matt. 1973. Distribution of solar radiation within a deciduous forest. Eastern Decid. Forest Biome Memo Rpt. No. 72-170, 26 p.
- Hutchison, B. A., and D. R. Matt. 1976. Beam en-

- richment of diffuse radiation in a deciduous forest. *Agric. Meteorol.* **17**:93-110.
- Kimball, H. H., and I. F. Hand. 1921. Sky brightness and daylight illumination measurements. *Am. Illum. Eng. Soc. Trans.* **16**:235-275.
- Matt, D. R., and B. A. Hutchison. 1974. Response of Lintronic Dome Solarimeters to varying solar radiation flux densities. US-IBP Eastern Deciduous Forest Biome Memo Rpt. No. 74-1, 8 p.
- Miller, E. E., and J. M. Norman. 1971. A sunfleck theory for plant canopies. II. Penumbra effect: Intensity distributions along sunfleck segments. *Agron. J.* **63**:739-743.
- Monteith, J. L. 1959. Solarimeter for field use. *J. Sci. Inst.* **36**:341-346.
- Moon, P., and D. E. Spencer. 1942. Illumination from a non-uniform sky. *Illum. Eng.* **37**:707-726.
- Niilisk, H., T. Nilson, and J. Ross. 1970. Radiation in plant canopies and its measurement, p. 165-177. In Prediction and measurement of photosynthetic productivity. Proc. of the IBP/PP Technical Meeting, Trebon, Czech. Center for Agricultural Publishing and Documentation, Wageningen, Netherlands.
- Norman, J. M., E. E. Miller, and C. B. Tanner. 1971. Light intensity and sunfleck-size distributions in plant canopies. *Agron. J.* **63**:743-748.
- Ovington, J. D., and H. A. I. Madgwick. 1955. Comparison of light in different woodlands. *Forestry* **28**: 141-146.
- Pokrowski, G. I. 1929. Über die Helligkeitsverteilung am Himmel. *Phys. Z.* **30**:697-700.
- Ramann, E. 1911. Lichtmessungen in Fichtenbestände. *Allg. Forst. Jagdztg.* **87**:401-406.
- Reifsnyder, W. E., G. M. Furnival, and J. L. Horowitz. 1971. Spatial and temporal distribution of solar radiation beneath forest canopies. *Agric. Meteorol.* **9**: 21-37.
- Salisbury, E. J. 1916. The oak-hornbeam woods of Hertfordshire, Parts I & II. *J. Ecology* **4**:83-117.
- Schomaker, C. E. 1968. Solar radiation measurements under a spruce and a birch canopy during May and June. *For. Sci.* **14**:31-38.
- Taylor, F. G. 1974. Phenodynamics of production in a mesic deciduous forest, p. 237-254. In H. Lieth [ed.] Phenology and seasonality modeling. Springer-Verlag, New York.
- Tsel'Niker, Y. L. 1968. Distribution of photosynthetically active radiation in the open and in the forest under various weather conditions, p. 33-337. In V. K. Pyldmaa [ed.] Actinometry and atmospheric optics. Translated from Russian by Israel Program for Scientific Translations, TT 70-505159, Vol. 8.
- Verhagen, A. M. W., J. H. Wilson, and E. J. Britten. 1963. Plant production in relation to foliage illumination. *Ann. Bot. (New Series)* **27**:627-640.